Supporting Information

Cell morphological profiling enables high-throughput screening for PROteolysis TArgeting Chimera (PROTAC) phenotypic signature

Maria-Anna Trapotsi[1,8], Elizabeth Mouchet[2], Guy Williams[2], Tiziana Monteverde[2], Karolina Juhani[2], Riku Turkki[3], Filip Miljković[4], Anton Martinsson[4], Lewis Mervin[5], Kenneth R. Pryde[6], Erik Müllers[7], Ian Barrett[8], Ola Engkvist[9], Andreas Bender[1], and Kevin Moreau[10*].

[1] Department of Chemistry, Centre for Molecular Informatics, University of Cambridge, Lensfield Road, Cambridge, CB2 1EW, UK

[2] High Throughput Screening, Discovery Sciences, BioPharmaceuticals R&D, AstraZeneca, Macclesfield, SK10 4TF, UK

[3] Data Sciences & Quantitative Biology, Discovery Sciences, BioPharmaceuticals R&D, AstraZeneca, Gothenburg, SE-43183, Sweden

[4] Imaging and Data Analytics, Clinical Pharmacology & Safety Sciences R&D, AstraZeneca, Gothenburg, SE-43183, Sweden

[5] Molecular AI, Discovery Sciences, BioPharmaceuticals R&D, AstraZeneca, Cambridge, CB2 0AA, UK

[6] Oncology Safety, Clinical Pharmacology and Safety Sciences R&D, AstraZeneca, Cambridge, CB2 0AA, UK.

[7] Bioscience Cardiovascular, Research and Early Development, Cardiovascular, Renal and Metabolism, BioPharmaceuticals R&D, AstraZeneca, Gothenburg, SE-43183, Sweden

[8] Data Sciences & Quantitative Biology, Discovery Sciences, BioPharmaceuticals R&D, AstraZeneca, Cambridge, CB2 0AA, UK

[9] Molecular AI, Discovery Sciences, BioPharmaceuticals R&D, AstraZeneca, Gothenburg, SE-43183, Sweden

[10] Safety Innovation, Clinical Pharmacology and Safety Sciences R&D, AstraZeneca, Cambridge, CB2 0AA, UK

***Corresponding author:** Kevin Moreau; kevin.moreau@astrazeneca.com

Supplemental information

Supplementary Figure 1: Structure of published PROTACs and non-PROTACs compounds, related to Figure 2.

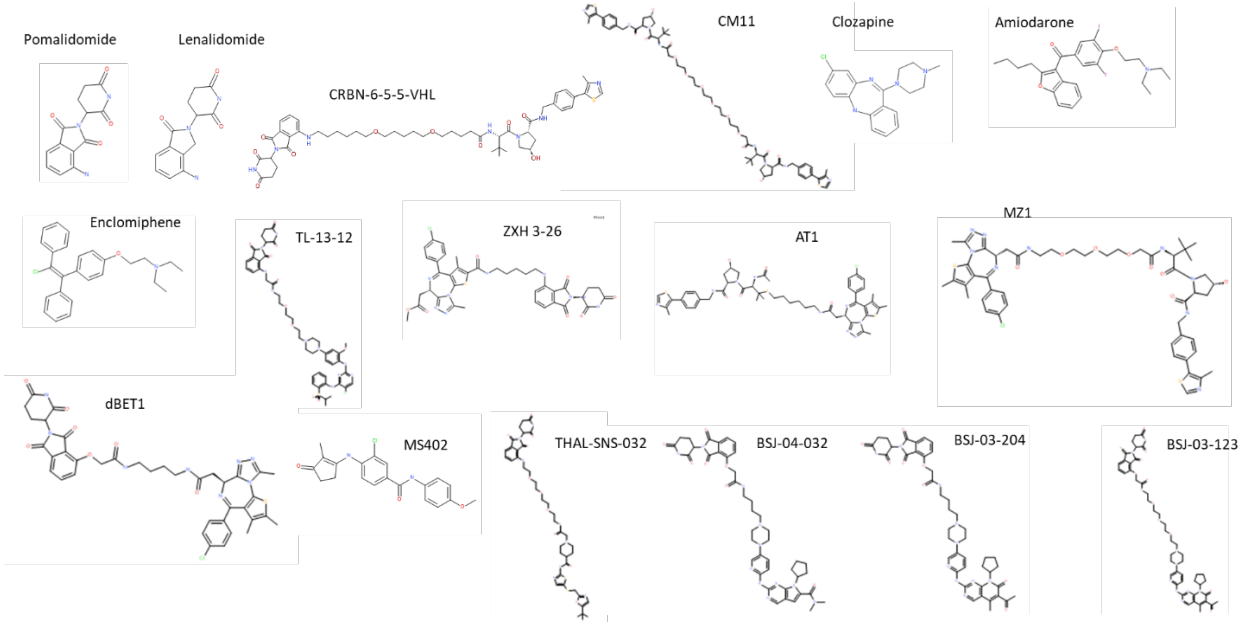

Supplementary Figure 2: Pearson correlation of PROTAC at different concentration. a) Pearson correlation values and b) median Pearson correlation of the image-based profiles for each PROTAC between concentrations 0.1 vs 1, 0.1 vs 10 and 1 vs 10 μM.

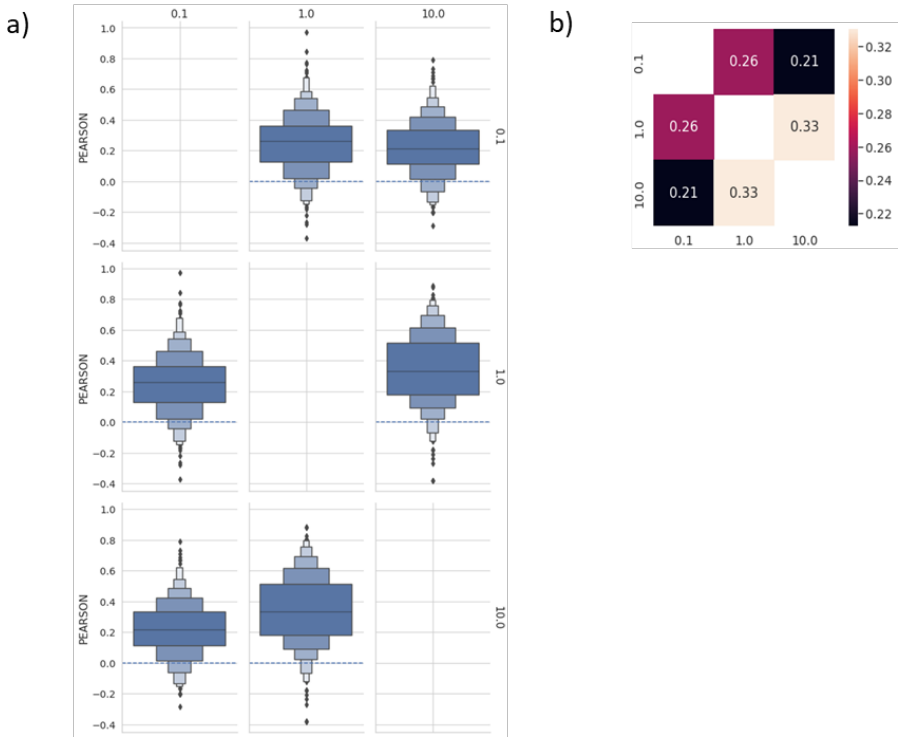

Supplementary Figure 3: Correlation Cell Painting activity versus primary target degradation. a) Correlation between primary degradation (pIC50) and Cell Painting Grit Score activity for all compounds or compounds with low/no target expression or compounds with target expressed. b) Correlation between primary degradation (pIC50) and Cell Painting Grit Score activity for Target 9, 11 and 14 with full dose response for 3 example compounds together with the Grit Score (GS). Related to Figure 3.

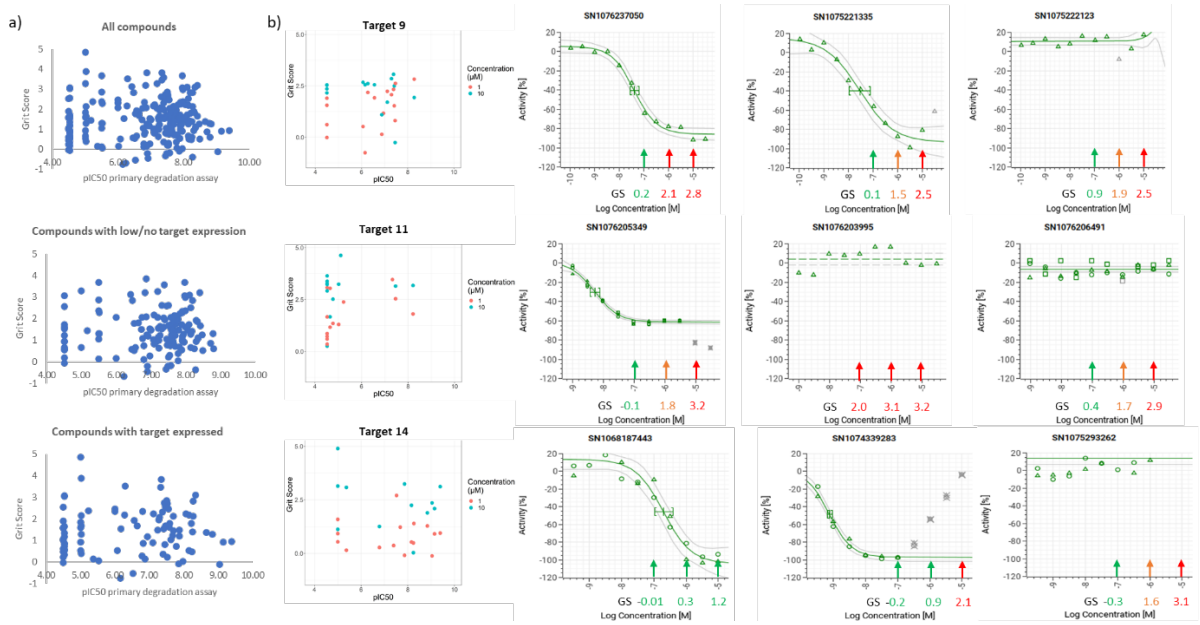

Supplementary Figure 4: Cell Painting activity for individual PROTAC components. a) Cell Painting activity score (Grit) for two PROTACs together with their corresponding part (E3 warheads and protein of interest POI ligands) and small molecules inhibitors b) Dose response of Gal assay for 2 compounds with Grit Score indication (GS). Related to Figure 4.

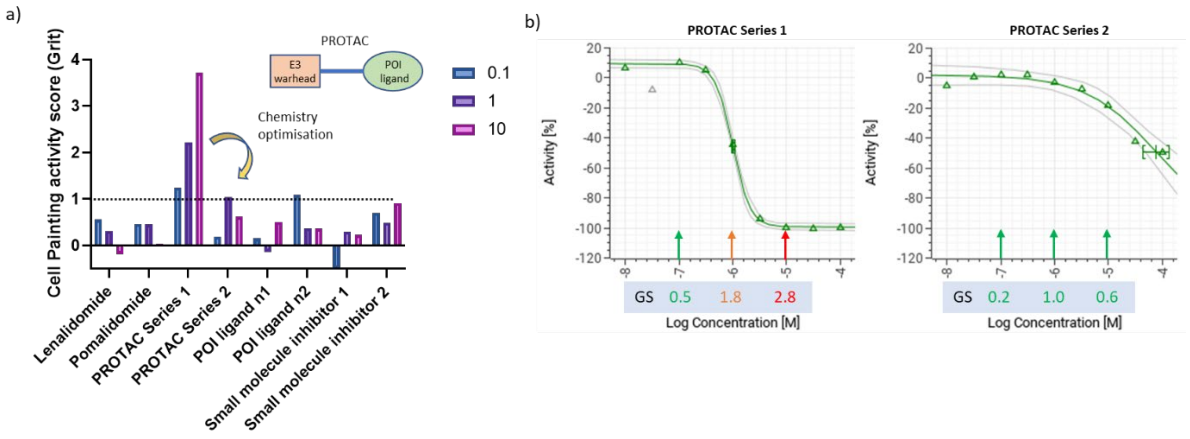

Supplementary Figure 5: Correlation Cell Painting activity versus mitotoxicity and phospholipidosis. a) Correlation Grit Score vs pIC50 in Gal assay at 0.1, 1 and 10 μM. b) Correlation Grit Score vs pIC50 in phospholipidosis (PLD) assay at 0.1, 1 and 10 μM. c) Correlation pIC50 in phospholipidosis (PLD) assay vs pIC50 in Gal assay. Related to Figure 5.

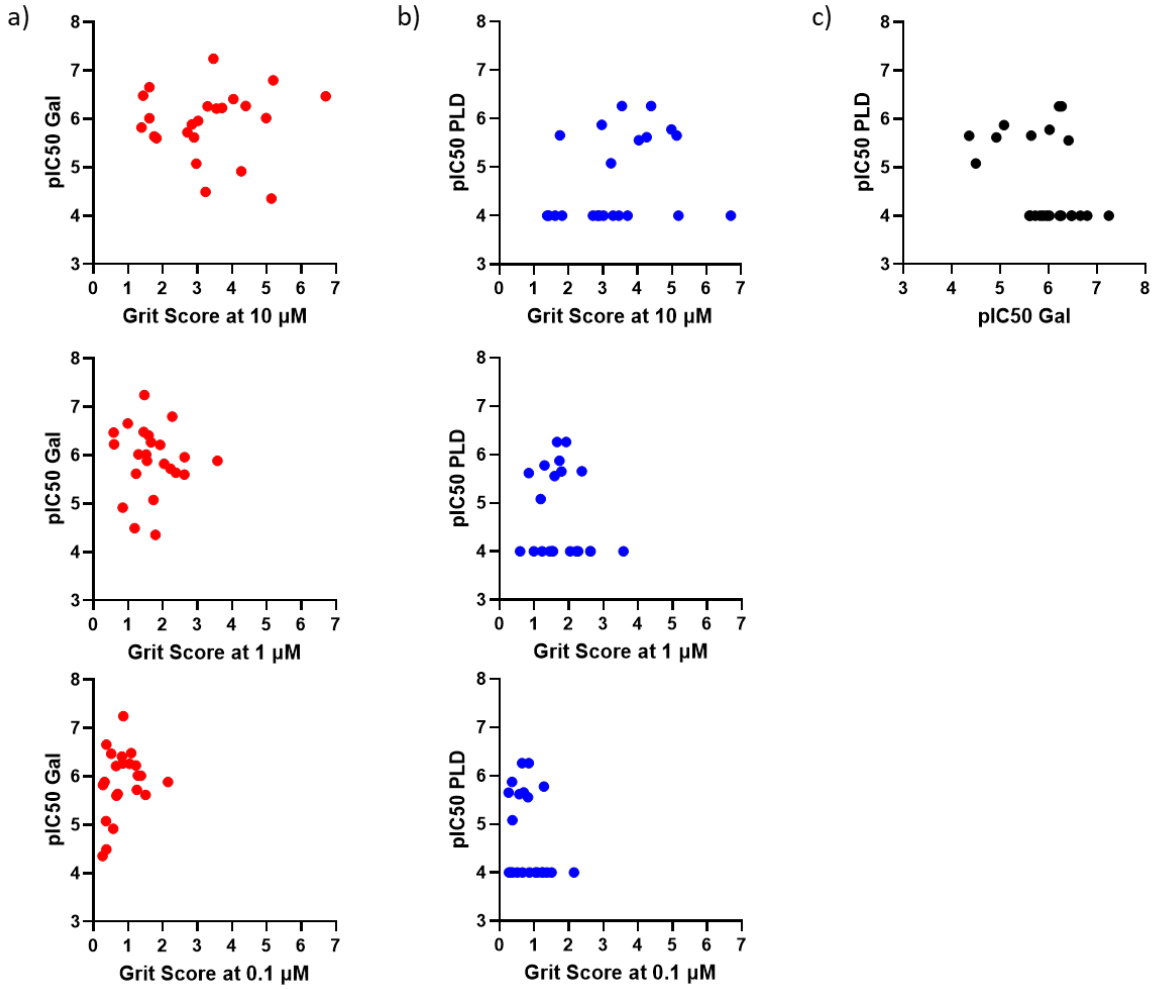

Supplementary Figure 6: Performance of y-scrambled models and Pairwise Pearson correlation. a) Performance of y-scrambled models for mitochondrial toxicity prediction using the Cell Painting features and three different algorithms; RF, XGB and SVC at concentrations 0.1, 1 and 10 μM. The error bars correspond to the confidence interval across all splits and random states used for cross validation. b) Pairwise Pearson correlation in the Cell Painting features space between the PROTACs in the external validation set and the compounds (PROTACs and non-PROTACs) in the mitochondrial toxicity models. The four following comparisons are performed. "New Mitotoxic vs Models' Mitotoxic" corresponds to the pairwise Pearson correlation calculation between the mitotoxic PROTACs in the external validation set and the mitotoxic compounds in the model. "New Mitotoxic vs Models' Not-Mitotoxic" corresponds to the pairwise Pearson correlation calculation between the mitotoxic PROTACs in the external validation set and the not-mitotoxic compounds in the model. "New Not-Mitotoxic vs Models' Mitotoxic" corresponds to the pairwise Pearson correlation calculation between the not mitotoxic PROTACs in the external validation set and the mitotoxic compounds in the model. "New Not-Mitotoxic vs Models' Not-Mitotoxic" corresponds to the pairwise Pearson correlation calculation between the not-mitotoxic PROTACs in the external validation set and the not-mitotoxic compounds in the model. These calculations are performed for concentration a) 0.1, b) 1 and c) 10 μM.

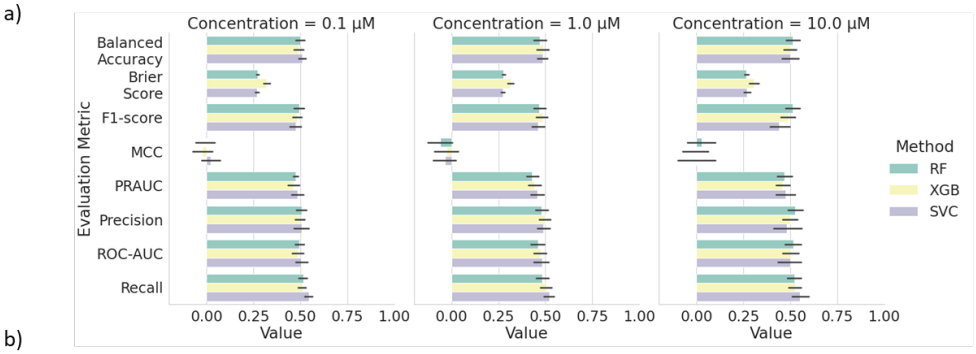

Supplementary Figure 7: Prospective experimental model validation results visualised with confusion matrices and model performance on the prospective validation set. a) Results obtained with the models trained with RF, SVC and XGB algorithms and with data from concentration 0.1,1 and 10 mM. b) Mitochondrial toxicity prediction performance using the Cell Painting features and three different algorithms; RF, XGB and SVC at concentrations a) 10, b) 1 and c) 0.1 μM. The error bars correspond to the confidence interval across all splits and random states used for cross validation.

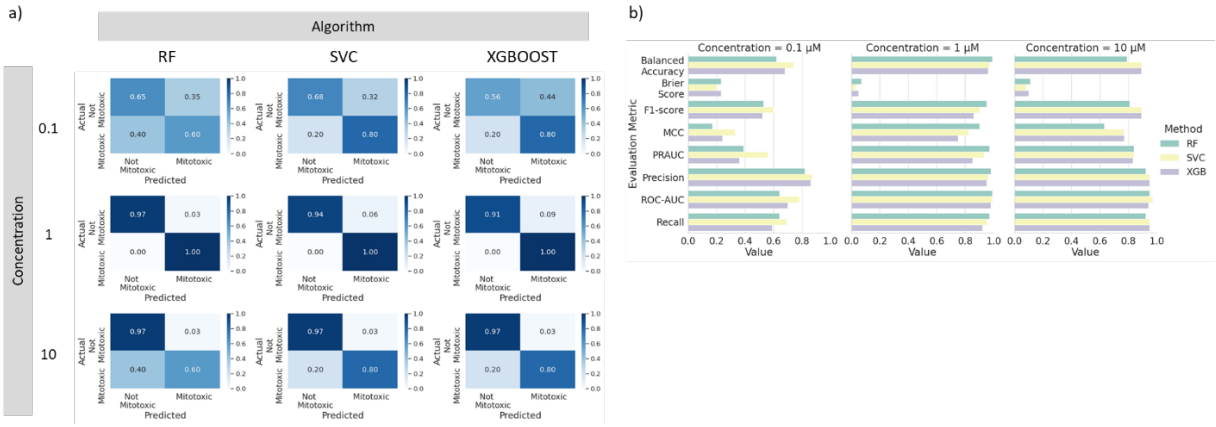

Supplementary Figure 8: Schematic representation of model training process. Initial data were partitioned in 70% train and 30% test set respectively, 5 times using the stratified shuffle split function from Scikit-Learn. The training set was further partitioned 5 times using the stratified shuffle split function from Scikit-Learn to identify the optimal hyperparameters using hyperopt and cross validation score function from Scikit-Learn. When hyperparameters were selected the models were trained and the compounds in the test set were predicted. This process was repeated with 3 different random seeds when the initial data were partitioned.

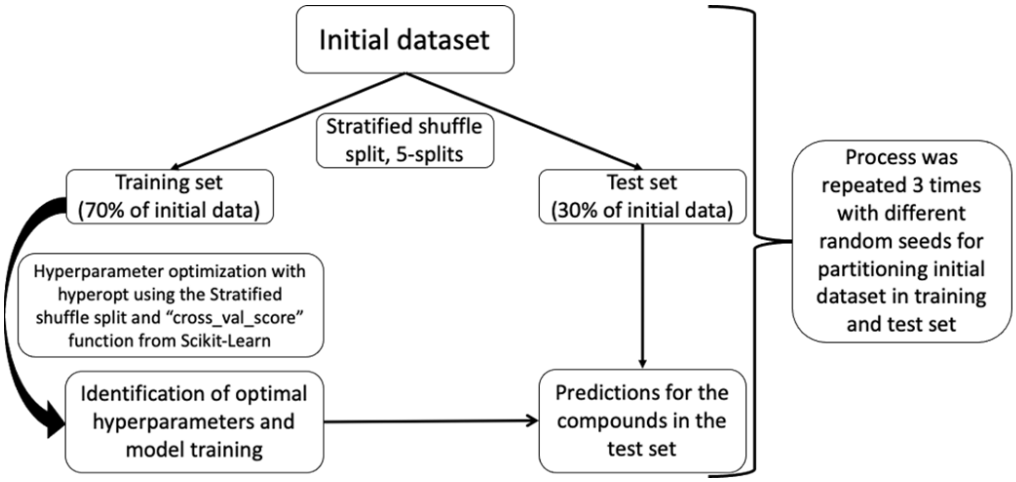

Supplementary Table 1: Considered machine learning hyperparameters. Range of hyperparameters' values considered for the RF, SVC and XGB algorithms. Hyperparameters were systematically evaluated using hyperopt python package.

Algorithm	Hyperparameter	Values
Random Forest	max_depth	3-50 with increments of 1
	n_estimators	100-1000 with increments of 100
	min_samples_split	2-50
	min_samples_leaf	1-15 with increments of 1
Support Vector Classifier (with rbf kernel)	gamma	10^{-10}-1
	C	10^{-4}-1000
eXtreme Gradient Boosting (XGB)	max_depth	3-18 with increments of 1
	n_estimators	100-1000 with increments of 100
	gamma	0-9
	reg_alpha	0.1-100 with increments of 1
	colsample_bytree	0-1
	min_child_weight	0-10 with increments of 1